academicJournals

Vol. 5(9), pp. 521-532, September 2013
DOI 10.5897/IJWREE12.121
ISSN 2141-6613 © 2013 Academic Journals
http://www.academicjournals.org/IJWREE

International Journal of Water Resources and Environmental Engineering

Full Length Research Paper

Using electronic signals and neural networks to monitor the performance of an anaerobic bioreactor

Willie F. Harper, Jr.[1]* and Taewoo Yi[2]

[1]Department of Systems Engineering and Management, Air Force Institute of Technology, Wright-Patterson Air Force Base, OH 45433 Korea.
[2]Department of Environmental Science and Engineering, Ewha Womans University, Seoul, 120-750 Korea.

Accepted 8 August, 2013

This study used a microbial fuel cell (MFC) and an artificial neural network (ANN) to monitor an anaerobic bioreactor (ANB) treating high strength wastewater. COD removal and methane production were observed and varied over the course of three operating stages. COD removal efficiency increased from 50 to 80% when nitrogen limitations were relieved. ANN processing of the electrical signals permitted the construction of an ANN that precisely predicted both the COD removal and methane production when 70% of the measured data was used for ANN training. This finding is notable given that there was no direct correlation between the signal metrics and ANB performance, and it is made more remarkable by the fact that electrical current represented approximately 1% of the overall ANB COD balance. This shows that ANN processing of small amounts of current can be used to predict the overall performance of an anaerobic bioreactor.

Key words: Anaerobic treatment, biosensing, microbial fuel cells, artificial neural networks.

INTRODUCTION

Anaerobic bioreactors (ANBs) usage is an attractive option for treatment of high strength wastewaters. The principle reasons for this are the lower energy and sludge production demands relative to aerobic systems, which translate into significantly lower costs and potentially lower long term environmental impacts (Speece, 1996). The production of methane is another key advantage because it can be harvested and used as an energy source (Metcalf and Eddy, 2003; Speece, 1996). ANBs are currently used to treat high strength wastewaters discharged from numerous industries, including breweries, dairy and cheese manufacturing, pulp and paper mills, and soft drink manufacturing (Metcalf and Eddy, 2003; Speece, 1996). As water reclamation facilities face growing concerns related to energy, climate change, and fiscal stress, ANB operations will require optimization in order to maximize the aforementioned benefits, and to this end, careful performance monitoring is essential.

ANBs can be monitored with microbial fuel cells (MFCs), devices that generate current and remove soluble organics by exploiting the activity of anaerobic bacteria that grow on (or near) an electrode surface. These anode-respiring bacteria (ARB) extract electrons from electron donors and donate them to the electrode surface. The electrons then travel through a wire and across an external resistor toward the cathode, where the terminal electron acceptor (usually oxygen) is reduced (Logan, 2007). Current is therefore tied to biological activity. Several researchers have shown that MFCs are appropriate biosensors (Kumlanghan et al., 2007; Di Lorenzo et al., 2009; Feng et al., 2011). Kumlanghan et al. (2007) showed that single-chamber MFCs produced a cell potential that correlate well with glucose levels in

*Corresponding author. E-mail: Willie.Harper@afit.edu. Tel: (937) 255-3636 ext 4528. Fax: (937) 937) 656-4699.

water samples and Di Lorenzo et al. (2009) showed that an air cathode MFC produced a linear relationship between COD concentration and current output. MFCs are promising biosensors, and they can be seamlessly integrated into ANBs with the goal of monitoring bioreactor performance in real time.

Recently, Feng and Harper (2013) used artificial neural networks (ANNs) to improve MFC-based biosensing. ANNs employ nonlinear (and sometimes linear) mathematical functions to map the relationship between input and output data. These models are especially for complex systems and when there are changing patterns (Dias et al., 2004; Yazici Ayse et al., 2007). ANNs connect input and output data with a series of hidden layers that contain neurons. Each neuron contains parameters that are trained with real data and then tested against a separate data subset. ANNs have also been combined with sensor arrays for detection of analytes (Ema et al., 1989; Gardner et al., 1990; Sundgren et al., 1991; Li et al., 1999). Using ANNs can therefore facilitate real-time monitoring of bioreactors, however, these models have never been used for monitoring ANBs.

The purpose of this study was to use MFC data to monitor the performance of an ANB. The hypothesis of this work is that ANNs can be used to correlate electrical signals with COD removal and methane production.

MATERIALS AND METHODS

Bioreactor operating conditions

The bioreactor was operated under anaerobic conditions, and it included a submerged MFC module and membrane filtration (Figure 1). The bioreactor had a 15 L of working volume. Dewatered sludge from an anaerobic digester was used as the inoculum for the MFC. The system was fully automated, with peristaltic pumps used to control the flow of influent, effluent, and backwash water. The pH was maintained between 7.0 to 7.2 using an automated controller (pH/ORP Controller, EUTECH Instruments Pte Ltd, Singapore) and pH electrode (Thermo Orion Glass pH electrode, Orion Research, INC. Beverly, MA). Alkalinity was added in the form of 1 M NaOH. The basin was mixed by re-circulating sludge with pneumatic pumps. The dissolved oxygen concentration in the basin was checked with a D.O. probe (ORION, Model 97-08-00) to confirm anaerobic conditions. The HRT was 15 days, the organic loading rate (OLR) was 1680g/m^3/day, and the SRT was 30 days. The temperature was typically 28°F, as confirmed with a thermometer. The influent COD was 25.2 g/L, and the primary substrates were acetate (19.5 g/L) and glucose (10.5 g/L). This feed solution was selected because many industries produce wastewaters with COD levels in this concentration range and because fermentable substrates are common (Hung et al., 1982; Hung, 1982; Kumaran et al., 1983; Luthy, et al., 1983; Satyawali and Balakrishnan, 2008). Nitrogen was added as NH_4Cl (44 mg/L as N, except during Stage 2 when N was added at 3.5 g/L as N). Phosphorus was added as KH_2PO_4 (10 mg/L as P). Additional minerals were added as $CaCl_2{\cdot}2H_2O$ (8 mg/L), Yeast extract (200 mg/L), $FeCl_3{\cdot}6H_2O$ (2 mg/L), $CoCl_2{\cdot}6H_2O$ (2 mg/L), $MnCl_2{\cdot}2H_2O$ (0.5 mg/L), $CuCl_2{\cdot}2H_2O$ (0.03 mg/L), $ZnCl_2$ (0.05 mg/L), H_3BO_3 (0.05 mg/L), $(NH_4)_6(Mo_7O_2)_4$ (0.09 mg/L), $NiCl_2{\cdot}6H_2O$ (0.05 mg/L), EDTA (1 mg/L), HCl (36%) (1 mL/L). This feed composition imposed both macro- and micro-nutrient limitations that were expected to limit both COD removal and methane production. The ultrafiltration membrane (ZeeWeed®-1 (ZW-1) Zenon Environmental) had 0.047 m^2 surface area, 0.04 µm pore size, and the operating flux was approximately 0.9 L/m^2/h. The pressure drop across the membrane was typically 0.5 psi or less. The membrane was backwashed four times daily using treated effluent. The air cathode MFC was submerged in the membrane reactor. The graphite anode was exposed to the anaerobic basin, while the cathode was exposed to a sealed, air-filled chamber which was separated from anaerobic basin by a cation exchange membrane (CEM) and the chamber walls.

Analytical methods

Soluble chemical oxygen demand was determined on aqueous samples according to Standard Methods (APHA, 1992). Samples were filtered using 0.45 µm glass microfiber filters (934-AH Whatman). Biogas was collected and measured by routing the gas stream into a water column and by measuring the displacement of the solution (Perez et al., 2001). The methane content of the biogas was measured by a GC/TCD (8500 Perkin Elmer) (APHA, 1992). The voltage associated with the MFC was measured using an autoranging multimeter (Sears, Roebuck, and Co., Model 82175, Hoffman Estates, Ill.). The external resistor was 1 k ohm. The current (mA) was calculated using ohms law, and the values were normalized (e.g. mW/m^2) using the cathode surface area.

Electrical signals and response metrics

In an effort to use the signals as a monitoring tool, each signal was described by two response metrics, the peak current (PC) and the pre-peak slope (PPS), which is a measure of how the current has changed in one day (Figure A.1). Each point on the electrical profile was used to calculate these two metrics in an effort to use them as input to the ANN.

Artificial neural network

ANNs were used to relate COD removal and methane production to the electrical response metrics. ANNs are mathematical models used to develop relationships between input and output data sets. A neural network is composed of an interconnected group of artificial neurons, where a neuron represents a point at which data is processed and then further propagated. A supervised, feed-forward network was customized with one-way connections between the input layer, the hidden layer(s), and the output layer. The neurons used the hyperbolic tangent sigmoid transfer function. Measured data was used for training. The Levenberg-Marquardt algorithm (LMA) was used (Marquardt, 1963). See Appendix B for more information about ANN structure and training.

Calculations of interest

The COD balance was calculated based on the following relationships:

$$COD_{rec} = COD_{eff} + COD_{sludge} + COD_{methane,\ gas} + COD_{methane,\ water} + COD_{current}$$

where, COD_{rec} is the mass of COD recovered (this should, in principle, be close to the influent COD), COD_{eff} is the effluent COD, COD_{sludge} is the COD associated with the sludge withdrawn from the reactor, $COD_{methane,\ gas}$ is the COD for gaseous CH_4. $COD_{methane,\ water}$ is the COD for methane dissolved in water (as estimated using Henry's Law), $COD_{current}$ is the COD converted to the current.

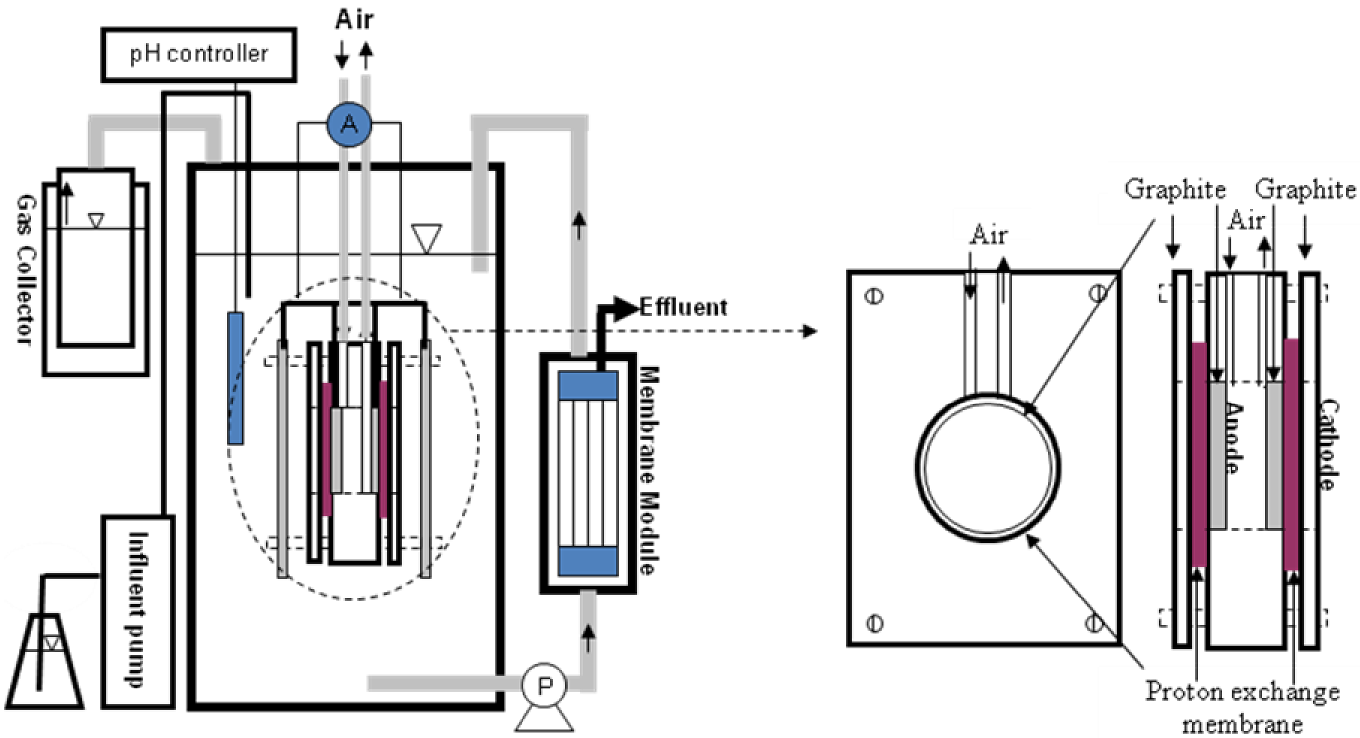

Figure 1. (a) Anaerobic membrane bioreactor with microbial fuel cell module (b) microbial fuel cell module.

$$1mA = \frac{8mgCOD - e^{-}eq}{96{,}485C} \qquad 1mLCH_4 = \frac{1mmolCH_4}{22.4mL}\,\frac{273.15K}{289.15K}\,\frac{8meqe^{-}}{mmolCH_4}\,\frac{8mgCOD}{meqe^{-}} = 2.7mgCOD$$

The Coulombic efficiencies (CEs) (%) are calculated as follows:

$$C_E = \frac{8It}{Fv_{An}\Delta COD}$$

Where F is Faraday's constant, v_{An} (L) is the working volume of the anode, ΔCOD (mg/L) is the COD removed, t is hydraulic retention time of the bioreactor.

RESULTS

Stage 1

The first operating stage corresponded to the operating period immediately following the initial inoculation of the MFC (Figure 2). During the first 10 operating days, the current density varied greatly, and on day 10 the current density decreased dramatically. At this point, the mixing intensity was improved, the electrodes were reinserted, and then the current density gradually increased. From day 11 to day 61, the current density increased from approximately 20 to 25 mA/m^2. This amounted to a 25% increase in current density. The COD removal efficiency during this stage was 60 to 80%, and the highest removal efficiencies occurred later in the operating period. Overall, gradual improvements in current density and COD removal were observed during Stage 1. The material balances retrieved during this operating period show that approximately 50% of the COD was recovered as methane, while effluent COD and withdrawn sludge accounted for the second and third largest COD sinks respectively (Figure A.2). Total recovery average approximately 90%. Current production accounted for < 1% of the recovered COD.

Stage 2

Stage 2 was the operating period immediately preceding and following nitrogen addition (Figure 3). After additional nitrogen was added, COD removal increased quickly from 50 to 80% over the course of 3 days. The gas generation also increased quickly from 2000 ml to 6000 ml. The current generation did not sharply increase, but there were incremental improvements in MFC output that were observed during the 3-day transient period and during the days that followed the nitrogen addition. The current density gradually increased by 25% after nitrogen addition. The coulombic efficiency (CE) decreased from 4

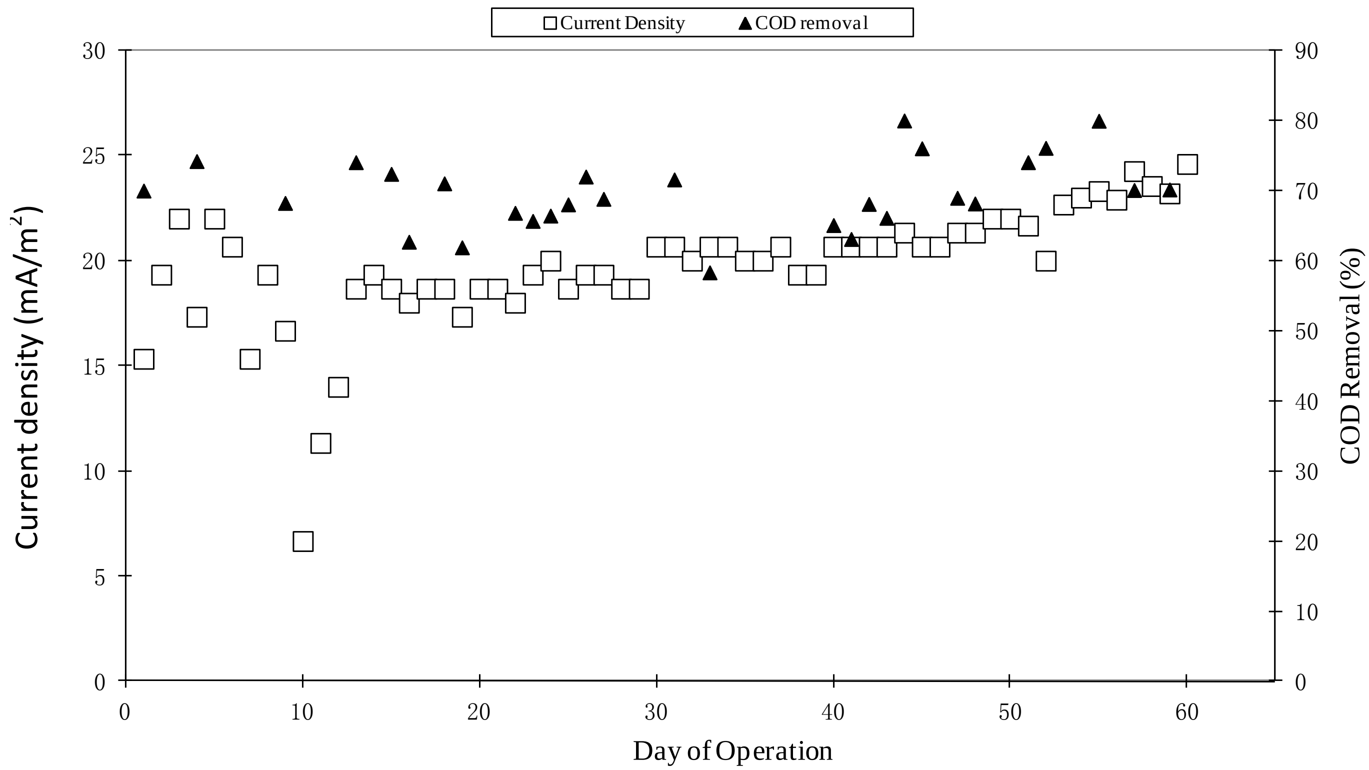

Figure 2. Performance and Current Generation, Stage 1.

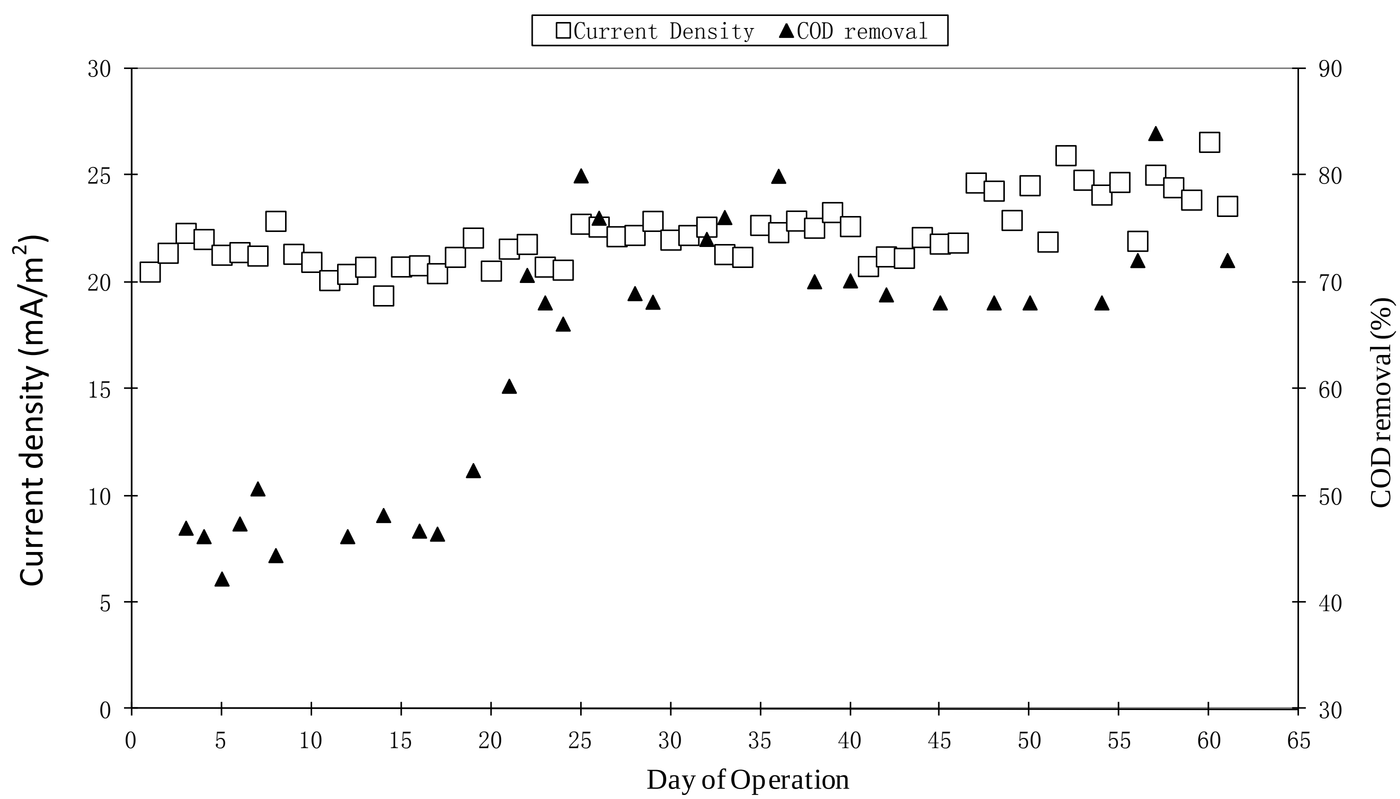

Figure 3. Performance and Current Generation,Stage 2.

to 1%. CE is related to the fraction of treated COD that is converted into current, and in this case, it decreased because the increase in COD removal did not translate into a proportional increase in current density. These results suggested that dramatic improvements in COD removal can have a gradual and modest impact on the output of the MFC. The material balances (Figure A.3) showed that nitrogen addition caused methane to become the most abundant COD sink, followed by effluent COD, and withdrawn sludge (current was a very low COD sink).

Stage 3

During stage treatment gradual treatment process deterioration was observed (Figure A.4). The COD removal efficiency decreased from 70 to 50% over a period of 80 days. The current density varied between 26 to 31 mA/m^2, but there were three notable current density measurements that were less than 25 mA/m^2. The measured gas generation also gradually decreased from 6000 to 4000 ml. The slow decline in COD removal, along with the relatively stable MFC output, caused the coulombic efficiency to increase from 1 to 3%. The process decline impacted the material balances (Figure A.5). Effluent COD initially accounted for approximately 25% of the COD balance but this fraction increased to 40%. The methane fraction decreased from 58 to 23% of the material balance. Withdrawn sludge accounted for 8 to 20% of the COD balance.

ANN modeling

The electrical signals were used to determine PC and PPS values. Neither of these two electrical metrics can be directly correlated to either COD removal or methane production because the relationships between these parameters involves many factors and is highly complex (Figure A.6 and A.7). However, ANNs are used to construct complex relationships. The trained ANN was used to predict the COD removal and methane production associated with a test data subset. The success of the ANN model depended on the amount of data used for ANN training (Figure 4). For example, when 70% of the experimental data was used for ANN training, the ANN precisely predicted the COD removal with just one hidden layer of neurons. The coefficients of determination (R^2) between the targets (that is, the actual measured COD removal percentages) and the ANN outputs (that is, the ANN-derived COD removal percentages) were 1. When 50 or 60% of the data was used, the ANN model performed very poorly and there were some ANN model outputs that were negative. Similar results were retrieved when the ANN model was used to predict methane production (Figure A.7). When 70% of the measured data is used, the correlations were precise, but when 50% or 60% of the data is used, the correlations were very poor. These findings show that electrical signals retrieved from a built-in MFC can be used to monitor the performance of an anaerobic bioreactor, and this success can be realized even when current represents a very small fraction of the COD balance.

DISCUSSION

The fundamental connection between methanogenesis and MFC activity has been the subject of previous research. When anodic electrodes are introduced into anaerobic bioreactors, the fate of the COD is impacted (Lee et al., 2008; Freguia et al., 2007). The effects documented by Lee et al. (2008) and Freguia et al. (2007) were more dramatic than those shown in the current study, because electrical current accounted for a large fraction of the electron equivalent sink. The current work departs from these previous studies by feeding a higher substrate concentration into a larger bioreactor volume (15 L, which yielded a smaller cathode surface area/reactor volume ratio, 0.04 cm^2/cm^3). In this case, current was a small fraction of the overall COD balance and the interactions between ARB, methanogens, and fermenting bacteria were more subtle as evidenced by the operational data. However, the ANN was used to unravel and then utilize the complexity of these ecological and biochemical relationships. Successful biosensor-based process monitoring can be accomplished using MFC current even when it is a small energy pool. Facilities should strongly consider augmenting anaerobic systems with MFCs to monitor process performance.

ANNs have been widely applied to map numerical relationships across a broad range of applications. These models enable predictive power in complex systems where the detailed mechanisms responsible for the relationships are usually poorly understood. As a result, there are many previous examples that show how ANNs have been used to map relationships between data sets that do not exhibit direct correlations (Dias et al., 2004; Yazici Ayse et al., 2007; Kumar et al., 2011). For example, ANNs can be used to predict evapotranspora-tion (ET) using atmospheric data like temperature, relative humidity, wind speed, and solar radiation, even though ET does not correlate well with any of the aforementioned parameters. Similar success has been realized with respect to the modeling of vehicular air emissions (Sharma et al., 2005) and renewable energy systems (Kalogirou et al., 2001). The current work falls in line with these previous efforts, because complex relationships were successfully mapped.

Conclusions

An ANB was augmented with a microbial fuel cell in order to monitor process performance with electrical data and

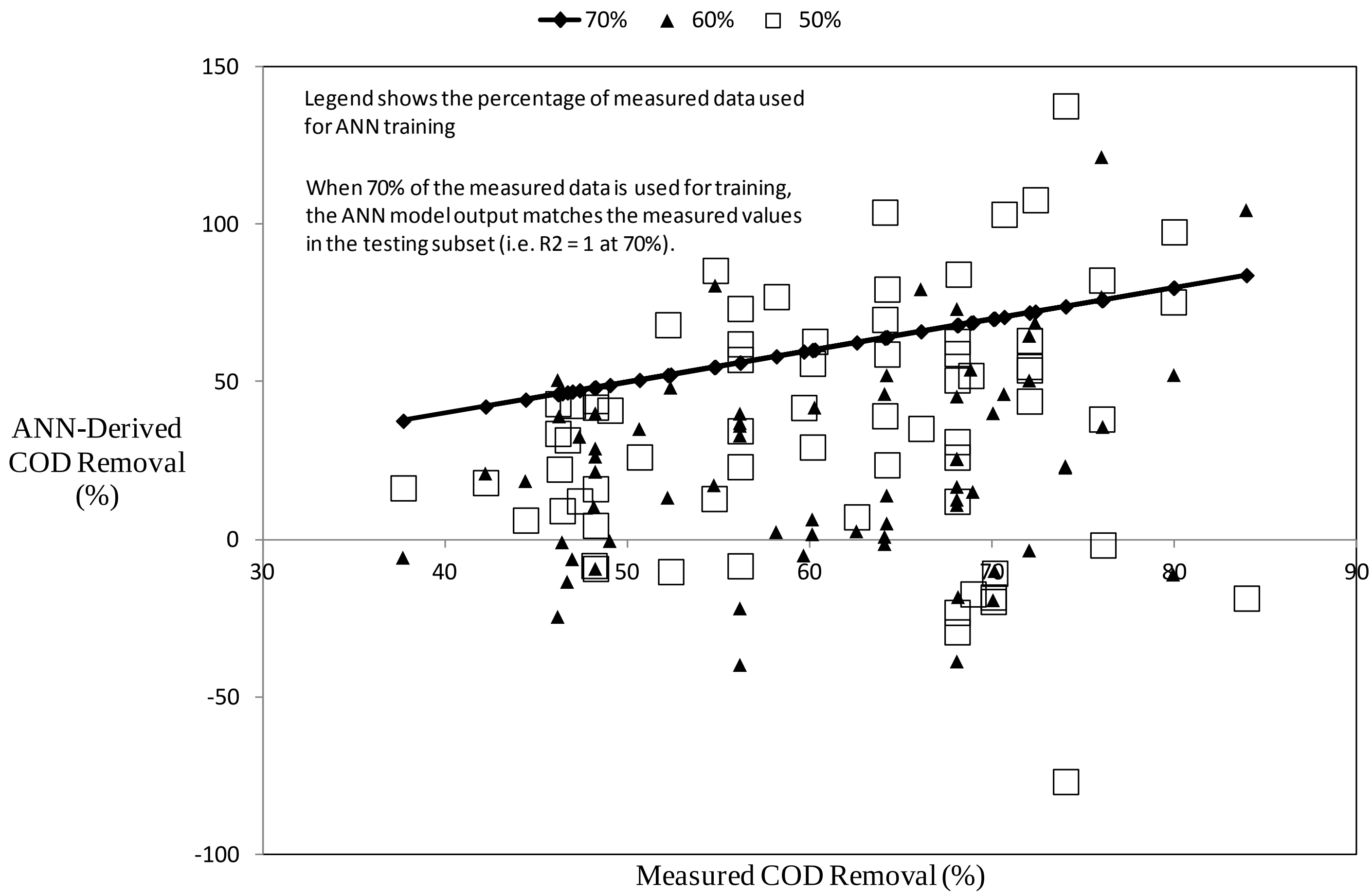

Figure 4. Effect of ANN training percentage on model performance, COD removal.

ANNs. COD removal and methane production were observed and varied over the course of three operating stages. COD removal efficiency was generally between 50 to 80%. Material balances showed that most of the COD was recovered as either methane or effluent COD. Current represented a small fraction of the recovered COD, but ANN processing of these small electrical signals allowed for precise correlations between process performance and ANN-derived predictions. This shows that ANBs can be accurately monitored with MFCs and ANNs.

ACKNOWLEDGEMENTS

The authors thank the National Science Foundation (NSF Grant No.BES-0827412) for financial support. The authors also thank Lin Wang for experimental assistance. The views expressed in this article are those of the authors and do not reflect the official policy or position of the Air Force Institute of Technology, United States Air Force, Department of Defense, or United States government.

REFERENCES

APHA, AWWA, WEF (1992). Standard Methods for the Examination of Water and Wastewater. Eighteenth Edition, Washington, D.C. p.1268.

Di Lorenzo M, Curtis TP, Head IM, Scott K (2009). A single-chamber microbial fuel cell as a biosensor for wastewaters. Water Res. 43:3145-3154.

Dias FM, Antunes A, Mota AM (2004). Artificial neural networks: A review of commercial hardware. Eng. Appl. Art. Intell. 17:945-952.

Ema K, Yokoyama M, Nakamoto T, Moriizuma T (1989). Odour-sensing system using quartz-resonator sensor array and neural network pattern recognition. Sens. Actuat. 18:291-296.

Feng Y, Kayode O, Harper WF (2013). Integration of microbial fuel cell output metrics and nonlinear modeling techniques for smarter biosensing. Sci. Total Environ. 449:223–228.

Freguia S, Rabaey K, Yuan Z, Keller J (2007). Electron and carbon balances in microbial fuel cells reveal temporary bacterial storage behavior during electricity generation. Environ. Sci. Technol. 41:2915-2921.

Gardner JW, Hines EL, Wilkinson M (1990). Application of artificial neural networks to an electronic olfactory system. Meas. Sci. Tech. 1:446-451.

Hung YT (1982). Evaluation of lignite liquefaction wastewater treatment by activated sludge process. Proceedings of the Second International Symposium held at the University of Waterloo, Waterloo, Ontario, Canada, June 18–20, 1980. In: Moo-Young, M., Robinson, C.W., Farquhar, G.J. (Eds.), Waste Treatment and Utilization, Theory and Practice of Waste Management, Part 2.

Hung YT, Fossum GO, Paulson LE, Willson WG (1982). Preliminary screening for the biological treatability of coal gasification wastewaters. Proceedings of the Second International Symposium held at the University of Waterloo, Waterloo, Ontario, Canada, June 18–20, 1980. In: Moo-Young, M., Robinson, C.W., Farquhar, G.J. (Eds.), Waste Treatment and Utilization, Theory and Practice of Waste Management, Part 2.

Kalogirou SA (2001). Artificial neural networks in renewable energy systems applications: A review. Renew. Sust. Energ. Rev. 5:373-401.

Kumar M, Raghuwanshi NS, Singh R (2011). Artificial neural networks approach in evapotranspiration modeling: A review. Irrig. Sci. 29:11-25.

Kumaran P, Kaul SN, Pandey RA, Choudary KR, Swarnakar NG, Parhad NM, Raman V (1983). Detoxification of phenol from LTC wastewater. IAWPC Technol. Annu. X:1–14.

Kumlanghan A, Liu J, Thavarungkul P, Kanatharana P, Mattiasson B (2007). Microbial fuel cell-based biosensor for fast analysis of biodegradable organic matter. Biosens. Bioelectron. 22:2939-2944.

Lee HS, Parameswaran P, Kato-Marcus A, Torres C, Rittmann BE (2008). Evaluation of energy-conversion efficiencies in microbial fuel cells utilizing fermentable and non-fermentable substrates. Water Res. 42:1501-1510.

Li Y, Brown CW, Sun F, McCrady JW, Traxler RW, Lo S (1999). Noninvasive fermentation analysis using an artificial neural network algorithm for processing near infrared spectra. Near Infrared Spec. 7:101–108.

Logan BE (2007). Microbial Fuel Cells. John Wiley & Sons Publishers, Hoboken, N.J., p. 200.

Luthy RG, Stamoudis VC, Campbell JR, Harrison W (1983). Removal of organic contaminants from coal conversion process condensates. J. Water Pollut. Control Fed. 55:196–207.

Marquardt D (1963). An algorithm for least-squares estimation of nonlinear parameters. SIAM J. Appl. Math. 11:431-441.

Metcalf L, Eddy HP (2003). Wastewater Engineering: Treatment and Reuse. McGraw-Hill Publishers, New York, NY. p. 1819.

Perez M, Romero L, Sales D (2001). Organic matter degradation kinetics in an anaerobic thermophilic fluidised bed bioreactor. Anaerobe, 7: 25-35.

Satyawali Y, Balakrishnan M (2008). Wastewater treatment in molasses-based alcohol distilleries for COD and color removal: A review. J. Environ. Manage. 86:481-497.

Sharma N, Chaudhry KK, Chalapati-Rao CV (2005). Vehicular pollution modeling using artificial neural network technique: A review. J. Sci. Ind. Res. 64:637-647.

Speece R (1996). Anaerobic biotechnology for industrial wastewaters. Archae Press Publishers, Nashville, TN., USA p..394.

Sundgren H, Winqulst F, Lukkari I, Lundstrom I (1991). Artificial neural networks and gas sensor arrays: Quantification of individual components in a gas mixture. Meas. Sci. Tech. 2:464-469.

Yazici Ayse C, Oegues E, Ankarali S, Canan S, Ankarali H, Akkus Z (2007). Artificial neural networks: Review. Turk. J. Med. Sci. 27:65-71.

APPENDIX A

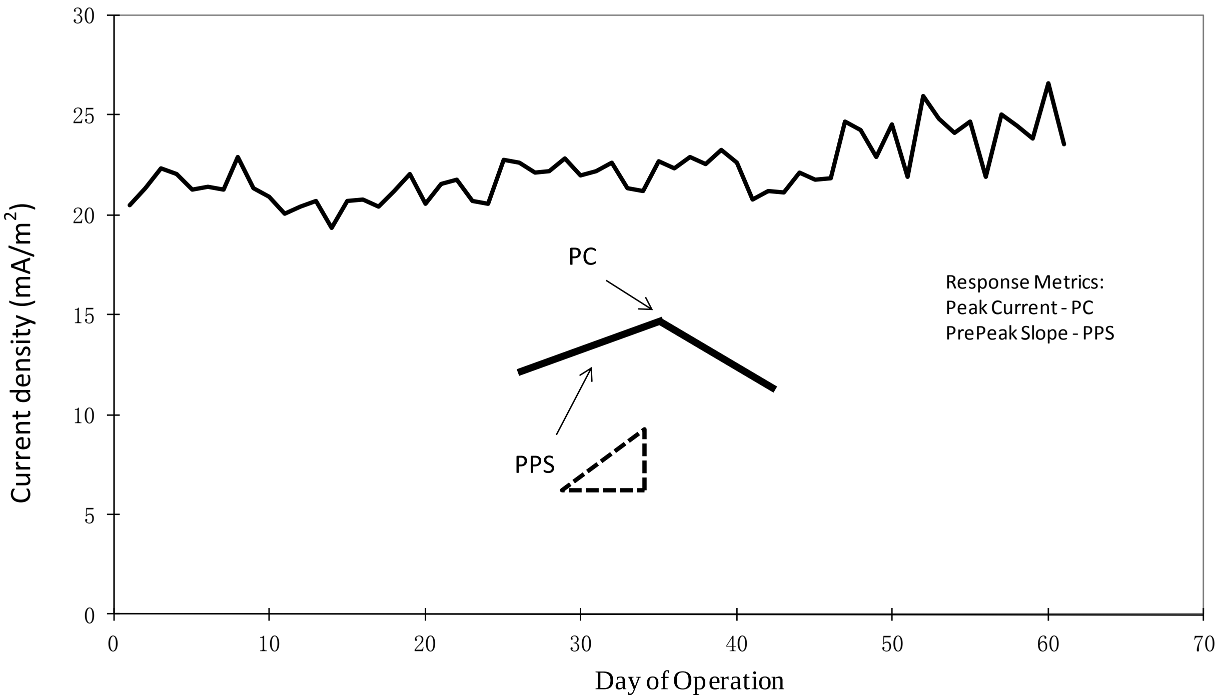

Figure A.1. Illustrating Response metrics.

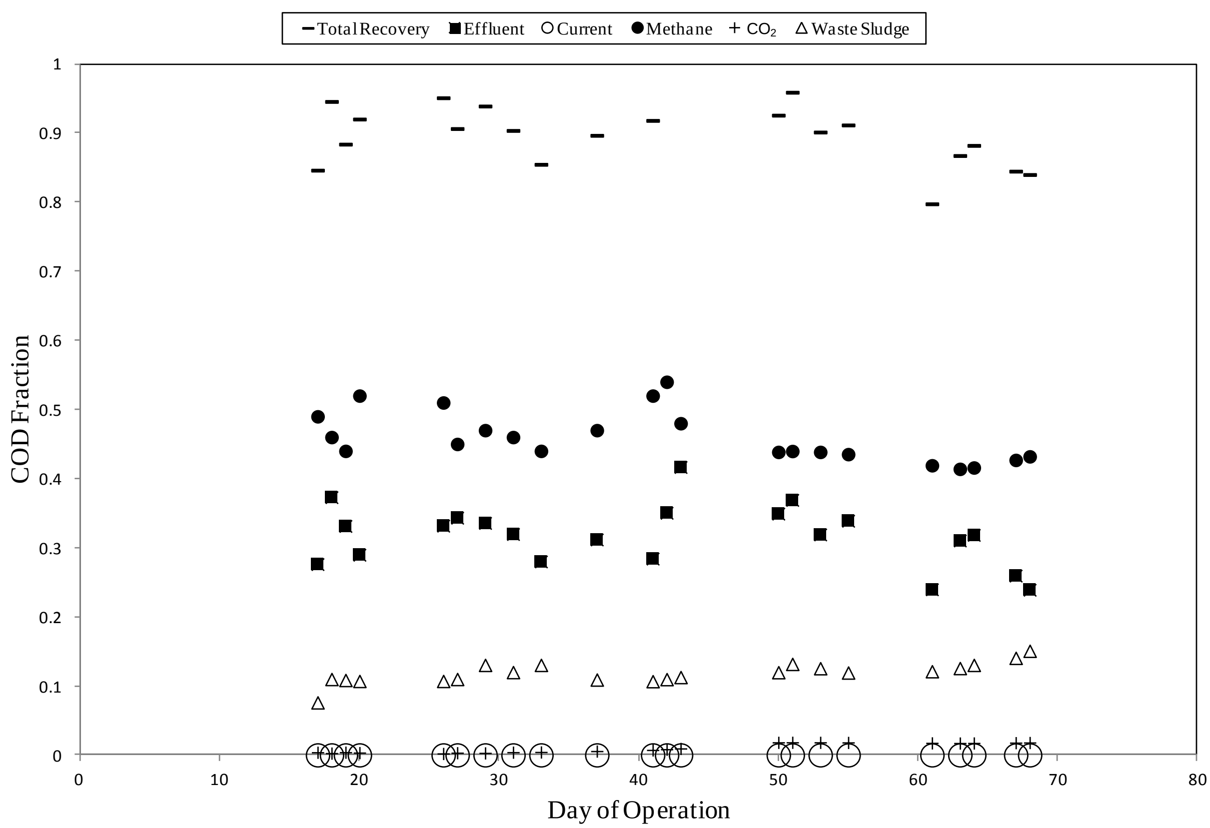

Figure A.2. Material balance during Stage 1.

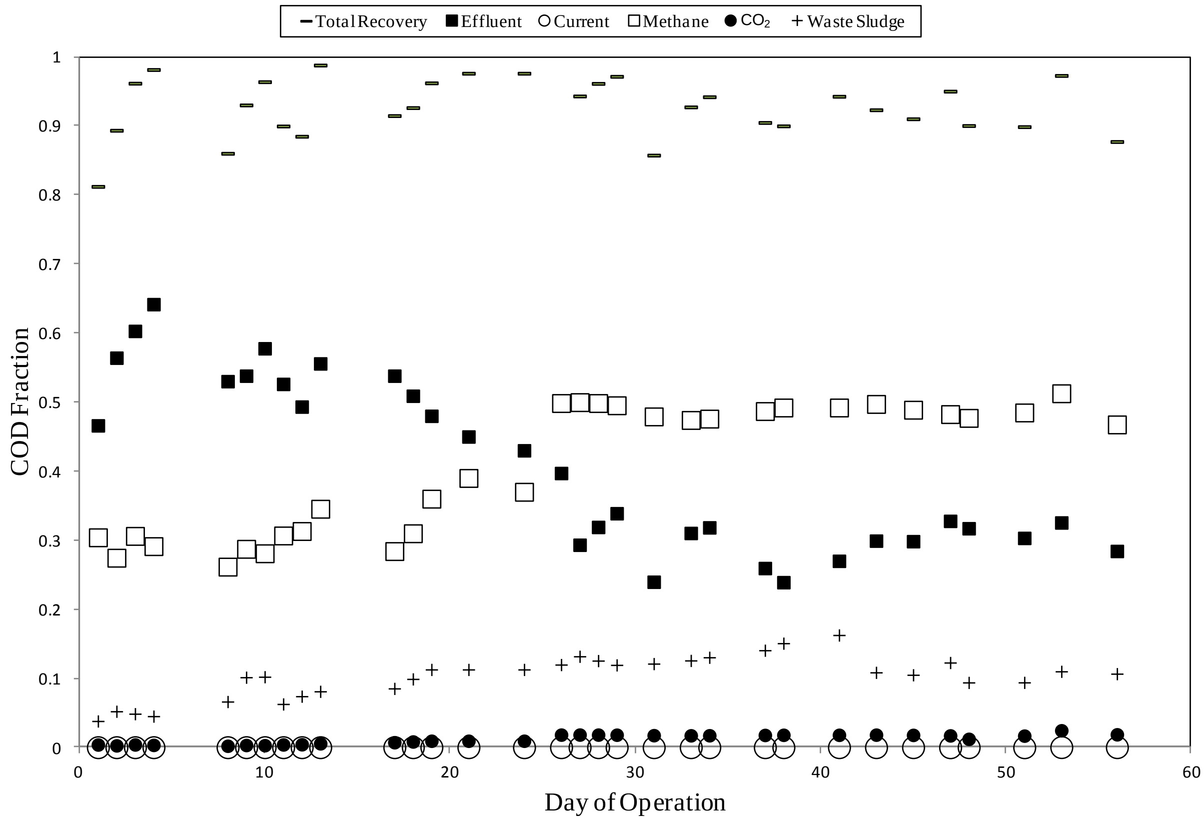

Figure A.3. Material balance during Stage 2.

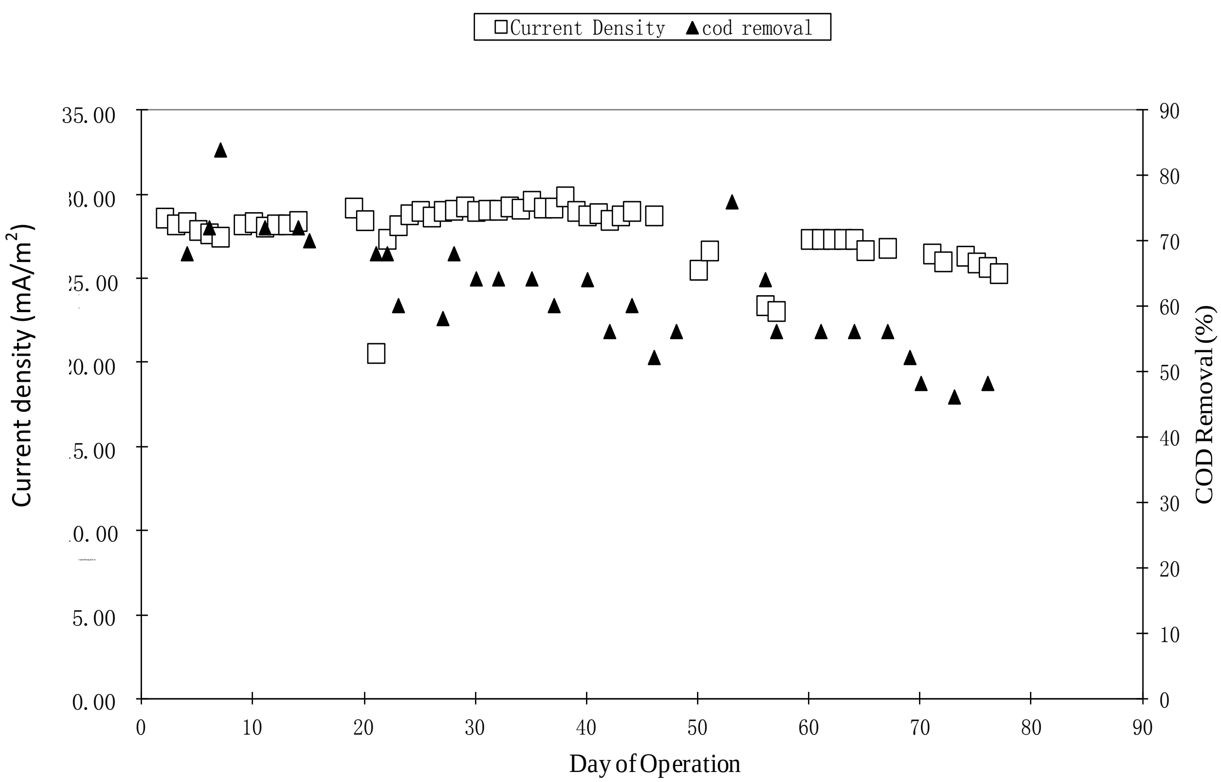

Figure A.4. Performance and Current generation (Stage 3).

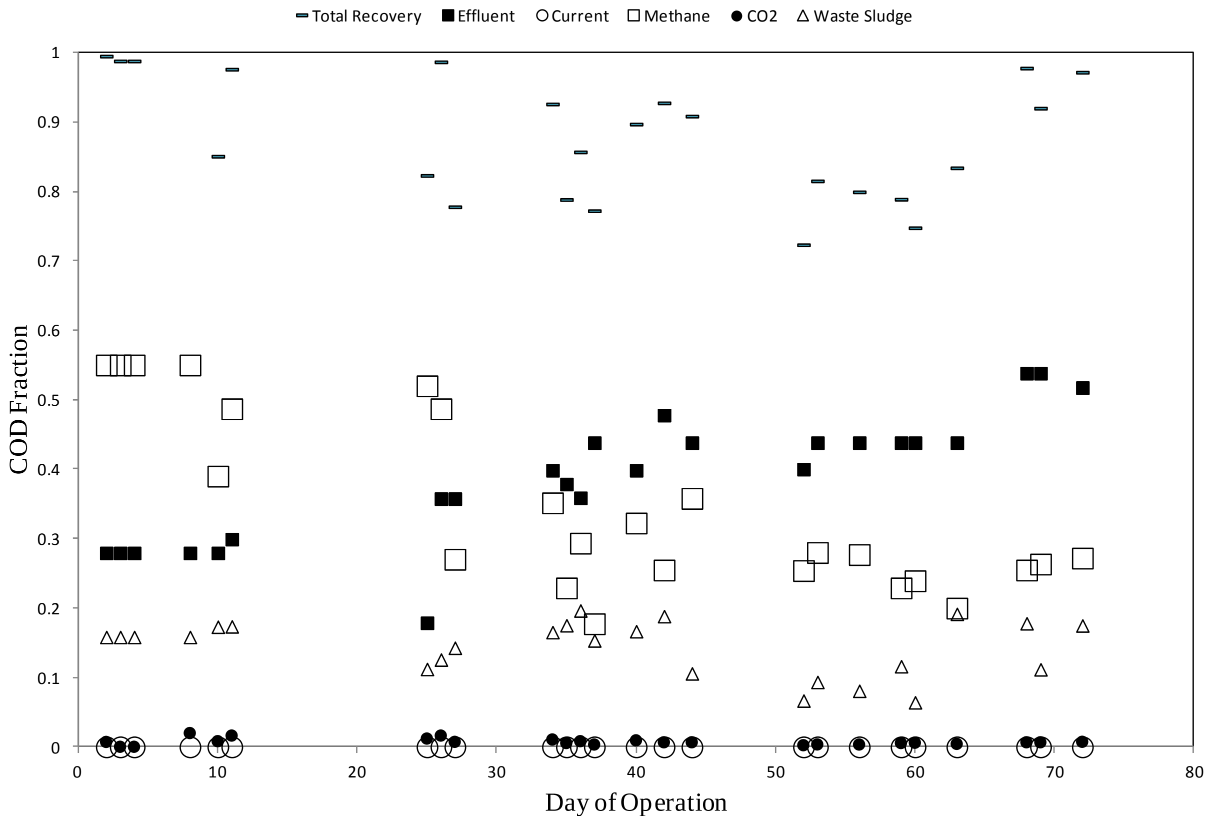

Figure A.5. Material balance during Stage 3.

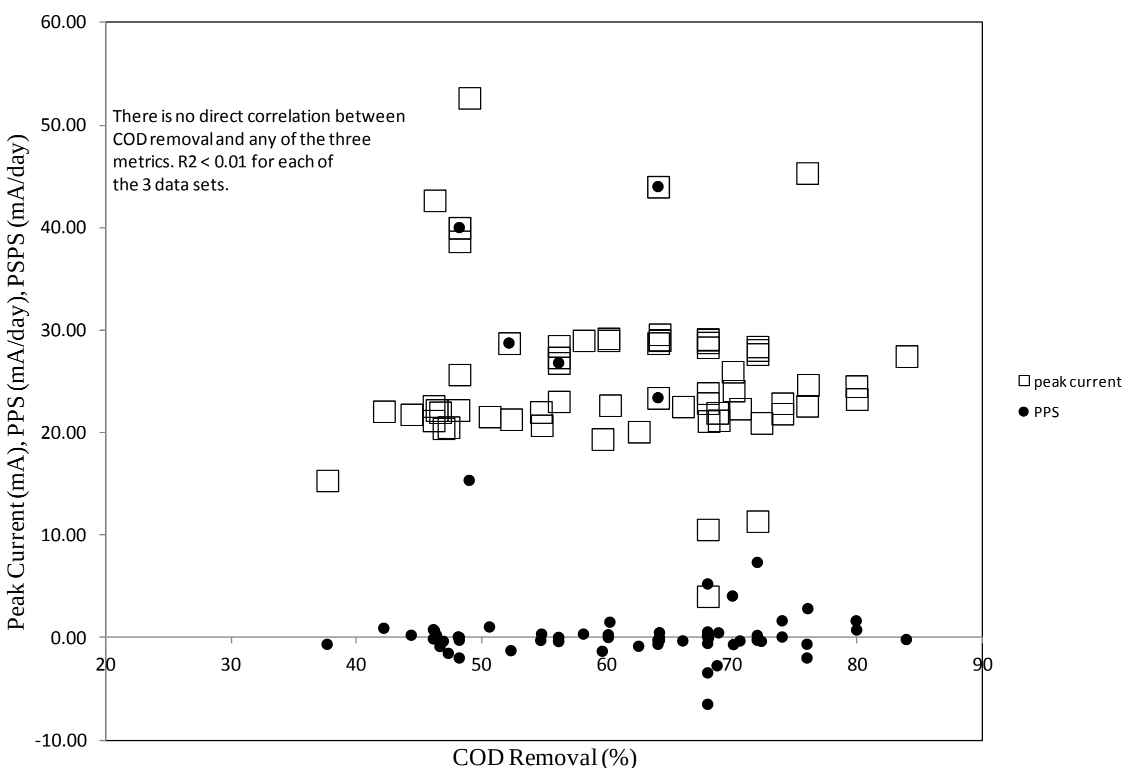

Figure A. 6. Correlations between COD Removal and the Response Metrics.

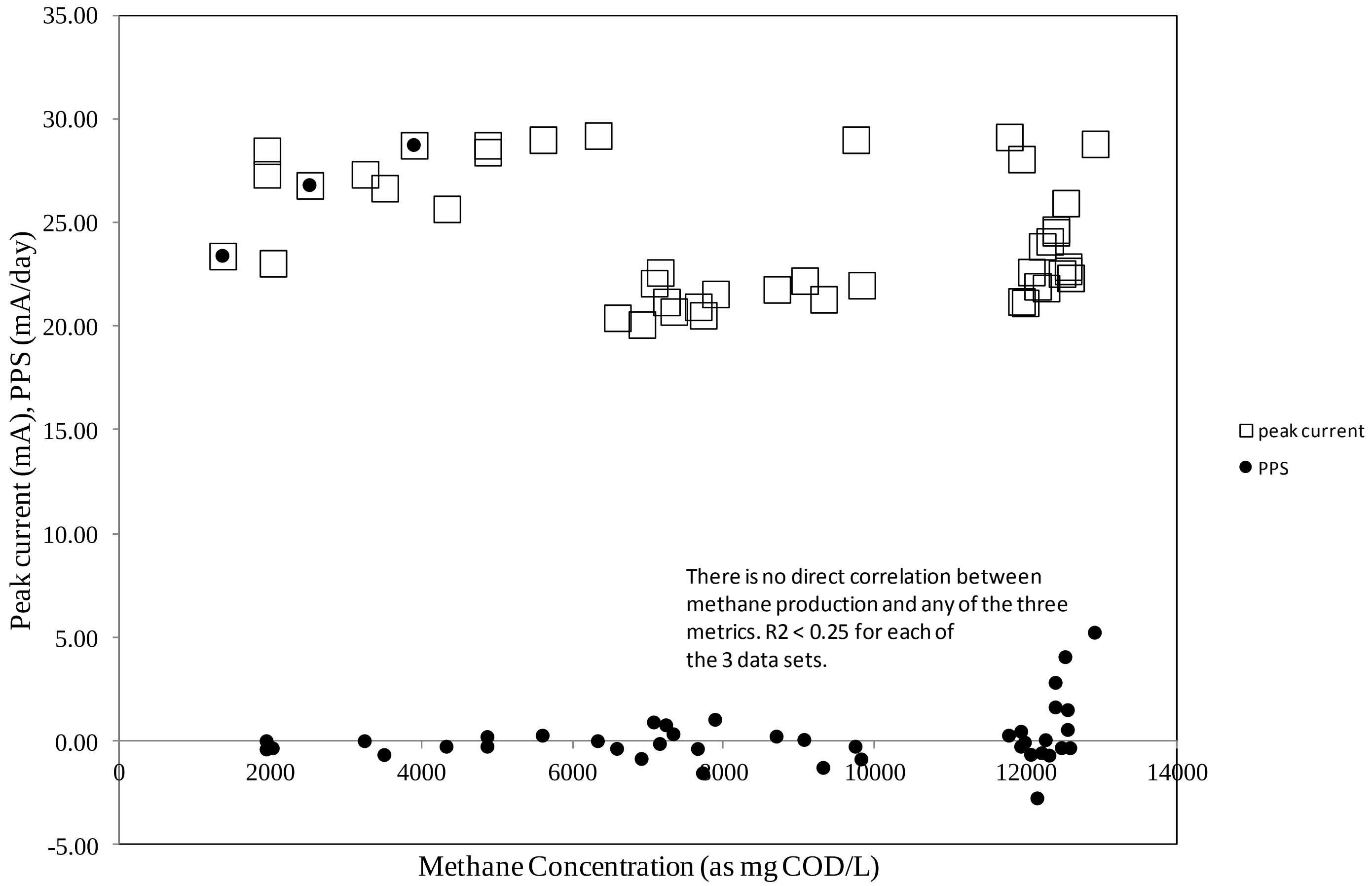

Figure A. 7. Correlations between Methane Production and the Response.

APPENDIX B

Supplemental information related to the artificial neural network: The Artificial Neural Network correlated COD removal and methane production to two metrics (that is, peak current, pre peak slope) related to the electrical signals. In general, the ANN has an input layer, output layer, and at least one hidden layer.

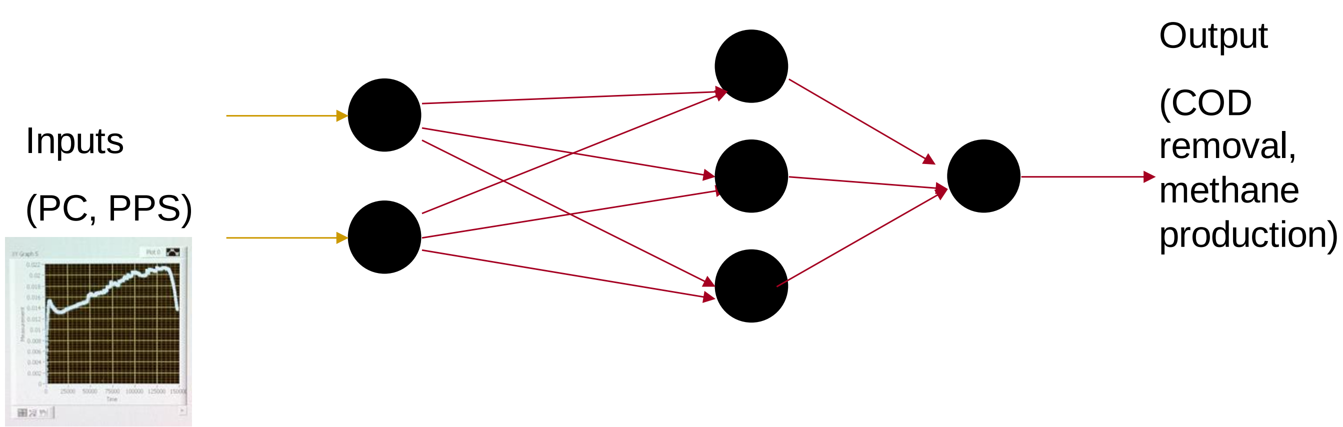

Figure B.1. Artificial neural network schematic: Each layer is composed of neurons. Each neuron uses a transfer function, numerical weights, and biases to propagate data through the network. During training, the proper weights and biases are determined for each neuron.

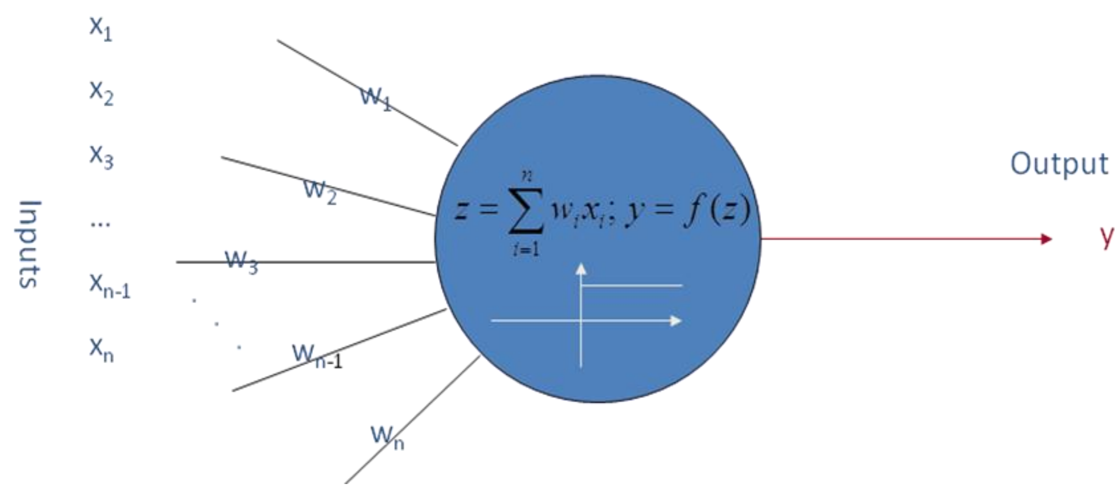

Figure B.2. Schematic of a neuron and the mathematical components: For the current work, the transfer function was the hyperbolic tangent sigmoid function. This function uses input data to compute the corresponding hyperbolic tangent according to the following: tansig(x_i) = 2/[1 + exp(-2 * x_i)) -1. The hyperbolic tangent sigmoid function is one of the default functions available on the MATLAB platform.

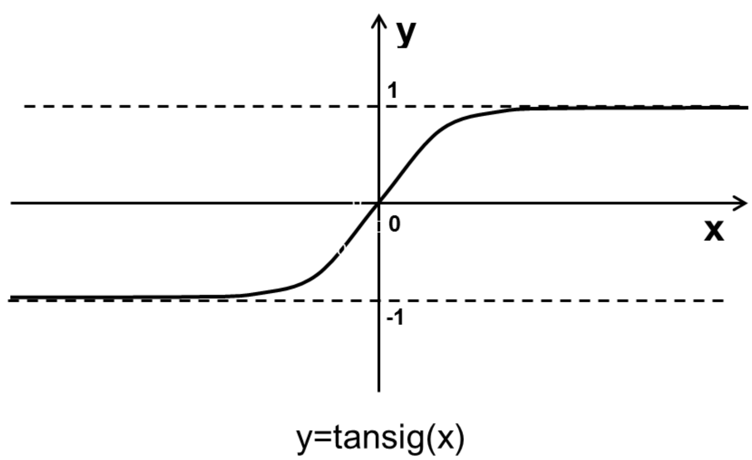

Figure B.3. The hyperbolic tangent sigmoid function: During training, the MATLAB interface reveals the performance of the system, as a function of the updated weights and biases associated with each neuron. During the training phase, the program first takes the input and propagates data forward to generate output. Then, there is back-propagation of the training pattern input in order to generate delta functions associated with the output and hidden neurons. The weights and biases are updated, and the propagation of data is repeated until #1) network performance (i.e. performance coefficient) is optimized, #2) the change in the network performance (i.e. the gradient coefficient) is minimized, #3) the number of iterations reached a maximum value, #4) the number of validation checks reaches a maximum value, #5) the network training method parameter (μ) reaches a maximum. The value of μ increases in value when there are large errors.